

# Spin Effects in the Local Density of States of GaAs

P. König, T. Schmidt, and R. J. Haug

*Institut für Festkörperphysik, Universität Hannover, Appelstr. 2, 30167 Hannover, Germany*  
(October 25, 2018)

We present spin-resolved measurements of the local density of states in Si doped GaAs. Both spin components exhibit strong mesoscopic fluctuations. In the magnetic quantum limit, the main features of the spin-up and spin-down components of the local density of states are found to be identical apart from Zeeman splitting. Based on this observation, we introduce a mesoscopic method to measure the  $g$ -factor in a material where macroscopic methods are severely restricted by disorder. Differences between the spin-up and spin-down components are discussed in terms of spin relaxation due to spin-orbit coupling.

Spin-polarized electronic transport is currently attracting a lot of interest from both a fundamental and an applied point of view [1]. Spin-polarized transport is essential for the operation of spin transistors or spin valves, and recently the spin injection from a ferromagnet into a semiconductor could be observed [2]. Spin effects have also been proposed to be utilized for quantum computation. In this respect it is important to study spin relaxation and coherence in semiconductors [3].

Particularly interesting spin phenomena were observed in mesoscopic semiconductor structures. Prominent examples are the Kondo effect in quantum dots [4,5] and spin-polarized tunneling through impurity levels. Resonant tunneling through impurities is also an established technique to image the local density of states (LDOS) of doped GaAs [7–10]. The LDOS exhibits mesoscopic fluctuations which can be understood in terms of interference of elastically scattered electron waves [7,8]. However, a spin-resolved measurement was impossible to date.

In this paper, we investigate the spin dependence of the LDOS via resonant tunneling through a spin-split impurity level. The strongest fluctuations of the spin-up and spin-down components of the LDOS are found to be identical apart from Zeeman splitting. This observation allows us to mesoscopically determine the  $g$ -factor in a material where macroscopic methods – such as photoluminescence or magnetotransport – are restricted by disorder. Differences between the spin-up and spin-down components are discussed in terms of spin relaxation due to spin-orbit coupling.

Our experiment is based on a strongly asymmetric double-barrier heterostructure, which was grown on  $n^+$ -type GaAs substrate. It consists of a 10 nm wide GaAs quantum well and two  $\text{Al}_{0.3}\text{Ga}_{0.7}\text{As}$  barriers of 5 and 8 nm width. The nominally undoped active region is sandwiched between 300 nm thick GaAs contact layers doped

with Si. The donor concentration has been experimentally determined to  $3.3 \times 10^{17} \text{ cm}^{-3}$  [8]. From this material we fabricated a 2  $\mu\text{m}$  diameter mesa with Ohmic contacts, which contains a small number of impurities in the quantum well.

We use the energetically-lowest impurity state  $S$  as spectrometer for the LDOS  $\nu$  in the emitter contact adjacent to the thick barrier, see Fig. 1. In a magnetic field  $B$ , the spectrometer exhibits a spin splitting  $\Delta E_S = g_S \mu_B B$ , with  $g_S$  the  $g$ -factor of the impurity and  $\mu_B$  the Bohr magneton. The spin splitting in the emitter is  $\Delta E = g \mu_B B$ . By applying a bias voltage  $V$ , the spin-split levels  $S_\uparrow$  and  $S_\downarrow$  are shifted in energy with respect to the emitter. They cross the Fermi level at  $V_{S_{\uparrow,\downarrow}} = (E_{S_{\uparrow,\downarrow}} - \mu_E^{ch})/e\alpha$  and two current steps result from resonant tunneling. Here,  $E_{S_\uparrow}$  and  $E_{S_\downarrow}$  are the energies of  $S_\uparrow$  and  $S_\downarrow$ ,  $\mu_E^{ch}$  is the chemical potential in the emitter (measured from the band edge in the well and emitter, respectively), and  $\alpha$  is the voltage-to-energy conversion coefficient. These two current steps can be clearly observed in Fig. 1(a), which shows the current-voltage characteristic  $I(V)$  of our device at the base temperature of  $T = 20$  mK of a dilution refrigerator. The spin splitting between the steps increases as  $B \parallel I$  is increased from 8.0 to 14.2 T. The overall shift of both steps to higher bias voltage is a consequence of the diamagnetic shift of  $E_S$  to higher energy.

As the tunneling rate of the thick emitter barrier is much lower than that of the collector barrier, the tunneling current images the LDOS in the emitter below the Fermi level  $\mu_E$  at the position of  $S$  [7]. If spin is conserved during tunneling, the current on the short plateau of the first step is proportional to the spin-up component of the LDOS,  $I_1 \propto \nu_\uparrow$ , while the current on the plateau of the second step reflects a superposition of both spin components,  $I_2 \propto \nu_\uparrow + \nu_\downarrow$ . At a bias voltage of  $V_{\uparrow,\downarrow} = (E_{S_{\uparrow,\downarrow}} - E)/e\alpha$ , the spin-up and spin-down components of the LDOS at energy  $E$  are probed by our experiment (measured from the band edge in the emitter). The oscillatory fine structure on the current plateaus in Fig. 1(a) reflects LDOS fluctuations in the heavily doped emitter [7]. These fluctuations are more pronounced in the numerically obtained differential conductance  $G = dI/dV$  shown in Fig. 1(b), where sharp peaks result from the current steps in the  $I(V)$  data.

To determine the  $g$ -factor of the spectrometer, we plot  $\Delta V_S = V_{S_\downarrow} - V_{S_\uparrow}$  as a function of magnetic field. Figure 2 shows that the data follows a straight line, which confirms that the two steps in the  $I(V)$  curves reflect one spin-split impurity level. From the temperature de-

pendence of the current step at  $B = 0$  T (not shown), we deduced a voltage-to-energy conversion coefficient of  $\alpha = 0.50$  for our device [6,11,12]. Using this value, we obtain  $|g_S| = e\alpha(d\Delta V_S/dB)/\mu_B = 0.14$ . The  $g$ -factor of the impurity is different from the bulk value due to a change of the electron energy as a result of the double-barrier confinement and the penetration of the electron wavefunction into the barrier material [14]. Note that the spin splitting of the spectrometer does not tell whether  $g_S$  is positive or negative.

Now we turn our attention to the LDOS in the magnetic quantum limit, in which only one spin-split Landau band remains populated in the emitter. The transition to this limit occurs at  $B \sim 11.4$  T. Figure 3(a) shows a color-scale image of the current as a function of bias voltage and magnetic field. It is dominated by two sharp current changes denoted by  $V_{S\uparrow}$  and  $V_{S\downarrow}$ , which reflect the spin-split steps in the  $I(V)$  curves in Fig. 1(a). The magnetic-field dependence of  $V_{S\uparrow}$  has been eliminated by shifting the  $I(V)$  curves in voltage. Between  $V_{S\uparrow}$  and  $V_{S\downarrow}$  as well as above  $V_{S\downarrow}$ , we observe pronounced fan-type resonances which reflect the local structure of Landau bands in the heavily doped emitter [8]. These resonances in the LDOS are formed by quasi-one-dimensional interference of multiply-scattered electron waves subject to Landau quantization. The slope of the LDOS resonances is  $dV_E/dB = 3.0$  mV/T [15].

To study the spin dependence of the LDOS, we define two cuts at  $V_1$  and  $V_2$  [dashed white lines in Fig. 3(a)]. Figure 3(b) shows the corresponding currents  $I_1$  and  $I_2$  as a function of magnetic field. Assuming in a first attempt that the spin-up and spin-down components of the LDOS in the emitter are identical apart from a Zeeman shift  $\Delta E$ , we can recalculate  $I_2(B)$  from  $I_1(B)$  as follows. From the sketch in Fig. 4, we deduce

$$I_1(B) \propto \nu_{\uparrow}(E_1, B) \quad (1)$$

and

$$I_2(B) \propto \nu_{\uparrow}(E_2, B) + \nu_{\downarrow}(E_2 + \Delta E_S, B) \quad (2)$$

where  $E_1$  and  $E_2$  correspond to  $V_1$  and  $V_2$  and  $\Delta E_S$  denotes the spin splitting of the spectrometer. Using  $\nu_{\downarrow}(E, B) = \nu_{\uparrow}(E - \Delta E, B)$ , we replace the spin-down component of the LDOS in Eq. (2) by its spin-up counterpart. In addition, we exploit the linear, fan-type character of the LDOS resonances and use  $\nu_{\uparrow}(E_1 + E, B) = \nu_{\uparrow}(E_1, B + [dB/dE_E]E)$  to rescale all energy values to  $E_1$ . Defining  $E_{21} = E_2 - E_1$ , we obtain

$$I_2(B) \propto \nu_{\uparrow} \left( E_1, B + \frac{dB}{dE_E} E_{21} \right) + \nu_{\uparrow} \left( E_1, B + \frac{dB}{dE_E} [E_{21} + \Delta E_S - \Delta E] \right) \quad (3)$$

from Eq. (2). Using Eq. (1), we now rewrite Eq. (3) into

$$I_2(B) = \gamma I_1 \left( B + \frac{dB}{dE_E} E_{21} \right) + \gamma I_1 \left( B + \frac{dB}{dE_E} [E_{21} + \Delta E_S - \Delta E] \right) . \quad (4)$$

Here,  $\gamma$  was introduced to compensate a difference in the coefficients of proportionality in Eqs.(1) and (2). It takes into account that the impurity can only be occupied by one electron at a time due to Coulomb interaction [6]. For our analysis, we estimate  $\gamma$  as  $\langle I_2 \rangle_B / 2 \langle I_1 \rangle_B = 0.98$  where  $\langle \dots \rangle_B$  symbolizes averaging over magnetic field. The slope  $dB/dE_E = 1/[e\alpha(dV_E/dB)] = 0.67$  T/meV and  $|g_S| = 0.14$  have been measured and, in a first step, we assume  $g = -0.44$  [13].

Figure 4 compares the experimental data for  $I_2$  with  $I_2^R$  recalculated according to Eq. (4). Assuming in addition  $g_S = -0.14$ , the strongest features in the LDOS are nicely reproduced by our reconstruction. Thus we conclude that the spin dependence of large fluctuations in the LDOS can be understood in terms of Zeeman splitting. These features vary slowly in magnetic field (on a scale of about 0.5 T or larger). The agreement also corroborates that both the spin-up and spin-down components of the LDOS are measured at the same location. The reconstruction does not work for  $g_S = +0.14$ , which strongly suggests that  $g_S < 0$  as predicted by calculations of the  $g$ -factor in a 10 nm wide quantum well [14,16]. Strong deviations between  $I_2$  and  $I_2^R$  are observed for features that vary rapidly in magnetic field (on a scale shorter than 0.1 T). This is more evident at the bottom of Fig. 4, where we plot  $\Delta I_2 = I_2 - I_2^R$  vs magnetic field.

In order to determine the actual  $g$ -factor in the heavily doped GaAs emitter, we minimize the root-mean-square deviation  $\sigma_{\Delta I_2} = \langle (\Delta I_2(B) - \langle \Delta I_2 \rangle_B)^2 \rangle_B^{1/2}$  with respect to  $g$ . Figure 5 shows a clear minimum at  $g = -0.35$ . The accuracy of  $g$  is limited by the uncertainty of  $g_S$ . Assuming an error of  $\pm 0.01$  in  $g_S$ , we calculate the error of  $g$  to be smaller than  $\pm 0.02$ . In our experiment, the  $g$ -factor is measured at the Fermi energy of about 25 meV above the band edge and at magnetic fields of 10.5 – 15 T, while the standard value  $g = -0.44$  was obtained at the band edge and at zero field [13]. The observed reduction of  $|g|$  is in accordance with theory predicting a reduction of the  $g$ -factor in high magnetic fields and at finite electron densities [17].

Now we address the origin of the difference between  $I_2$  and  $I_2^R$  in Fig. 4. One issue to be considered is energy relaxation. The “holes” generated by tunneling in the emitter Fermi sea have an energy deficit  $e\alpha(V - V_{S\uparrow,\downarrow})$  with respect to  $\mu_E$  (see sketch in Fig. 1). The higher the bias voltage the larger is this energy deficit, resulting in a faster relaxation via electron-electron scattering. Inelastic scattering reduces the phase-coherence length in the emitter and thus suppresses the LDOS fluctuations. This effect is clearly visible in Fig. 1, where the fluctuations become less pronounced with increasing bias volt-

age. Similarly one might expect that  $I_2$  is different from  $I_2^R$ , since  $I_2$  is measured deeper below the Fermi level than  $I_1$  which is used to calculate  $I_2^R$ . To check this idea, we calculated  $\Delta I_2 = I_2 - I_2^R$  for  $0.5 \text{ mV} \leq V_2 \leq 1 \text{ mV}$  corresponding to an energy range of  $0.25 \text{ meV}$ . Interestingly,  $\Delta I_2$  is fairly independent from  $V_2$ , which demonstrates that energy relaxation is irrelevant in our experiment.

Thus the difference between  $I_2$  and  $I_2^R$  either indicates an inaccuracy in our reconstruction – possibly resulting from a magnetic-field dependence of the parameters  $\gamma$ ,  $dB/dE_E$ ,  $g_S$ ,  $g$  – or it gives evidence of additional spin effects beyond Zeeman splitting. While we will not be able to give a definite answer, it is worth while to examine the influence of extra spin effects on the LDOS.

One possibility is spin relaxation due to spin-orbit coupling in the emitter [3]. In this case, we can estimate the spin-relaxation time as follows. Semiclassically speaking, the LDOS fluctuations are a result of quantum interference of diffusive electron waves at length scales between the mean free path and the phase-coherence length [7]. Long interference paths correspond to weak features that vary rapidly in magnetic field. By calculating the differential conductance  $G = dI/dV$ , we favor small and rapid variations resulting from long interference paths [see Fig. 1(b)]. Due to the limited energy resolution  $\hbar\Gamma$  of our spectrometer, the longest and dominant length scale in the conductance is  $l_\Gamma = \sqrt{D/\Gamma}$ , where  $D$  is the diffusion constant in the emitter [7,18]. The correlation magnetic field of the conductance fluctuations is

$$B_{c,G} \sim \phi_0/l_\Gamma^2 = \phi_0/(D/\Gamma) . \quad (5)$$

By calculating the difference  $\Delta I_2 = I_2 - I_2^R$ , we eliminate the spin-independent features of the LDOS. Hence the correlation magnetic field of the fluctuations in  $\Delta I_2$  contains information about spin relaxation,

$$B_{c,\Delta I_2} \sim \phi_0/l_s^2 = \phi_0/D\tau_s , \quad (6)$$

with  $l_s = \sqrt{D\tau_s}$  being the spin-relaxation length. From Eqs. (5) and (6), we now calculate the spin-relaxation time

$$\tau_s \sim (B_{c,G}/B_{c,\Delta I_2})/\Gamma . \quad (7)$$

All parameters in this expression have been measured in our experiment. In particular, it does not depend on the diffusion constant. From the measured  $G(B)$  and  $\Delta I_2(B)$  data we find  $B_{c,G} \sim 0.01 \text{ T}$  and  $B_{c,\Delta I_2} \sim 0.03 \text{ T}$  (in analogy to Ref. [7]), and from the width of the conductance peaks in Fig. 1(b) we deduce an energy resolution of  $\hbar\Gamma \approx e\alpha \times 80 \mu\text{V} \approx 40 \mu\text{eV}$ . Using these values, we obtain a spin-relaxation time of  $\tau_s \sim 5 \text{ ps}$ . It is much longer than the elastic scattering time  $\tau = 0.1\text{--}0.2 \text{ ps}$ , which we determined according to Ref. [18].

Another interesting spin effect may result from the presence of magnetic impurities in the emitter. The exchange field of fully spin-polarized impurities leads to different disorder potentials for spin-up and spin-down

electrons and thus influences the LDOS [19]. As there may only be residual magnetic impurities, their density will be by orders of magnitude lower than the Si concentration. Therefore, the spin-dependent features of the disorder potential vary on longer length scales than the spin-independent features. Slow variations in space correspond to small features on short field scales in the LDOS. Thus a small amount of magnetic impurities could explain why small features in the LDOS exhibit an irregular spin dependence, while large features simply show a regular Zeeman splitting. To clarify the influence of magnetic impurities on the LDOS, we suggest to deliberately dope the GaAs contacts of a double-barrier heterostructure with magnetic impurities such as Mn [20].

In summary, we used a spin-split impurity level as spectrometer to study the interplay of Zeeman splitting and disorder in Si doped GaAs via resonant tunneling. Both the spin-up and spin-down components of the LDOS show fan-type resonances as a consequence of Landau quantization in the bulk semiconductor. While the main resonances in the LDOS exhibit a Zeeman shift that can be best described using a  $g$ -factor of  $g = -0.35$ , the smaller resonances show a complicated irregular behavior. Spin relaxation due to spin-orbit coupling is one possible origin of this deviation from Zeeman splitting.

We gratefully acknowledge A. Förster and H. Lüth for growing the double-barrier heterostructure and V.I. Fal'ko for useful discussions.

- 
- [1] For a review, see G. A. Prinz, *Science* **282**, 1660 (1998).
  - [2] P. R. Hammar *et al.*, *Phys. Rev. Lett.* **83**, 203 (1999).
  - [3] See, for example, D. D. Awschalom and J. M. Kikkawa, *Physics Today* **52**, No. 6, 33 (1999).
  - [4] D. Goldhaber-Gordon *et al.*, *Nature* **391**, 156 (1998).
  - [5] S. M. Cronenwett, T. H. Oosterkamp, and L. P. Kouwenhoven, *Science* **281**, 540 (1998).
  - [6] M. R. Deshpande *et al.*, *Phys. Rev. Lett.* **76**, 1328 (1996).
  - [7] T. Schmidt *et al.*, *Europhys. Lett.* **36**, 61 (1996).
  - [8] T. Schmidt *et al.*, *Phys. Rev. Lett.* **78**, 1540 (1997).
  - [9] M. R. Deshpande *et al.*, p. 1899 in *22nd International Conference on the Physics of Semiconductors*, edited by D. J. Lockwood (World Scientific, Singapore, 1995); J. W. Sleight *et al.*, *Phys. Rev. B* **53**, 15727 (1996).
  - [10] The LDOS in two-dimensional electron gases was studied by P. J. McDonnell *et al.*, *Physica B* **211**, 433 (1995), *Solid State Electron.* **40**, 409 (1996), and T. Ihn *et al.*, *Physics Uspekhi* **41**, 122 (1998).
  - [11] B. Su, V. J. Goldman, and J. E. Cunningham, *Phys. Rev B* **46**, 7644 (1992).
  - [12] A. K. Geim *et al.*, *Phys. Rev. Lett.* **72**, 2061 (1994).
  - [13] C. Weisbuch and C. Hermann, *Phys. Rev. B* **15**, 816 (1977).
  - [14] E. L. Ivchenko and A. A. Kiselev, *Sov. Phys. Semicond.* **26**, 827 (1992); A. A. Kiselev, E. L. Ivchenko and U.

- Rößler, Phys. Rev. B **58**, 16353 (1998).
- [15] In Fig. 3(a), the slopes of the spin-up and spin-down resonances are slightly different due to the spin splitting of the impurity level. However, this effect is negligible [ $d\Delta V_S/dB = 0.02$  mV/T  $\ll$   $dV_E/dB = 3.1$  mV/T].
- [16] The sign of the  $g$ -factor of self-assembled quantum dots was determined by A. S. G. Thornton *et al.*, Appl. Phys. Lett. **73**, 354 (1998).
- [17] M. Braun and U. Rößler, J. Phys. C **18**, 3365 (1985); P. Pfeffer and W. Zawadzki, Phys. Rev. B **41**, 1561 (1990).
- [18] V. I. Fal'ko, Phys. Rev. B **56**, 1049 (1997).
- [19] At the low temperatures of our experiment, any magnetic impurities will be fully spin-polarized such that spin-flip scattering of electrons at these impurities is unlikely.
- [20] H. Ohno, Science **281**, 951 (1998).

FIG. 1. (a) Current-voltage curves  $I(V)$  measured at  $B = 8.0$  T (solid) and 14.2 T (dashed) at  $T = 20$  mK. (b) Differential conductance  $G = dI/dV$  numerically obtained from the  $I(V)$  curves. The sketch shows the spin-resolved local density of states (left) in the emitter of a double-barrier heterostructure (shown to the right).

FIG. 2. Spin splitting  $\Delta V_S = V_{S\downarrow} - V_{S\uparrow}$  of the spectrometer vs magnetic field.

FIG. 3. (Color). (a) Color map of the current vs bias voltage (step  $7$   $\mu$ V) and magnetic field  $B \parallel I$  (step  $10$  mT) for  $T = 20$  mK (white,  $I \leq 0.0$  nA; black,  $I \geq 0.5$  nA). The raw data has been shifted in voltage such that the first current step defines origin of the voltage scale. The image is dominated by fan-type resonances  $V_E$ . (b) Current vs magnetic field at  $V_1$  (dashed,  $I_1$ ) and  $V_2$  (solid,  $I_2$ ).

FIG. 4. Reconstruction of  $I_2$  from  $I_1$ : Comparison of the measured current  $I_2$  (solid) with the reconstructed current  $I_2^R$  (dashed). The solid line at the bottom shows the difference  $\Delta I_2 = I_2 - I_2^R$  as a function of magnetic field. The sketch shows the local density of states (left) and the spectrometer position for  $V_1$  and  $V_2$  (right) to illustrate the reconstruction principle. Annotations are described in the text.

FIG. 5. Root-mean-square deviation  $\sigma_{\Delta I_2}$  of  $\Delta I_2 = I_2 - I_2^R$  as a function of the  $g$ -factor in the emitter.

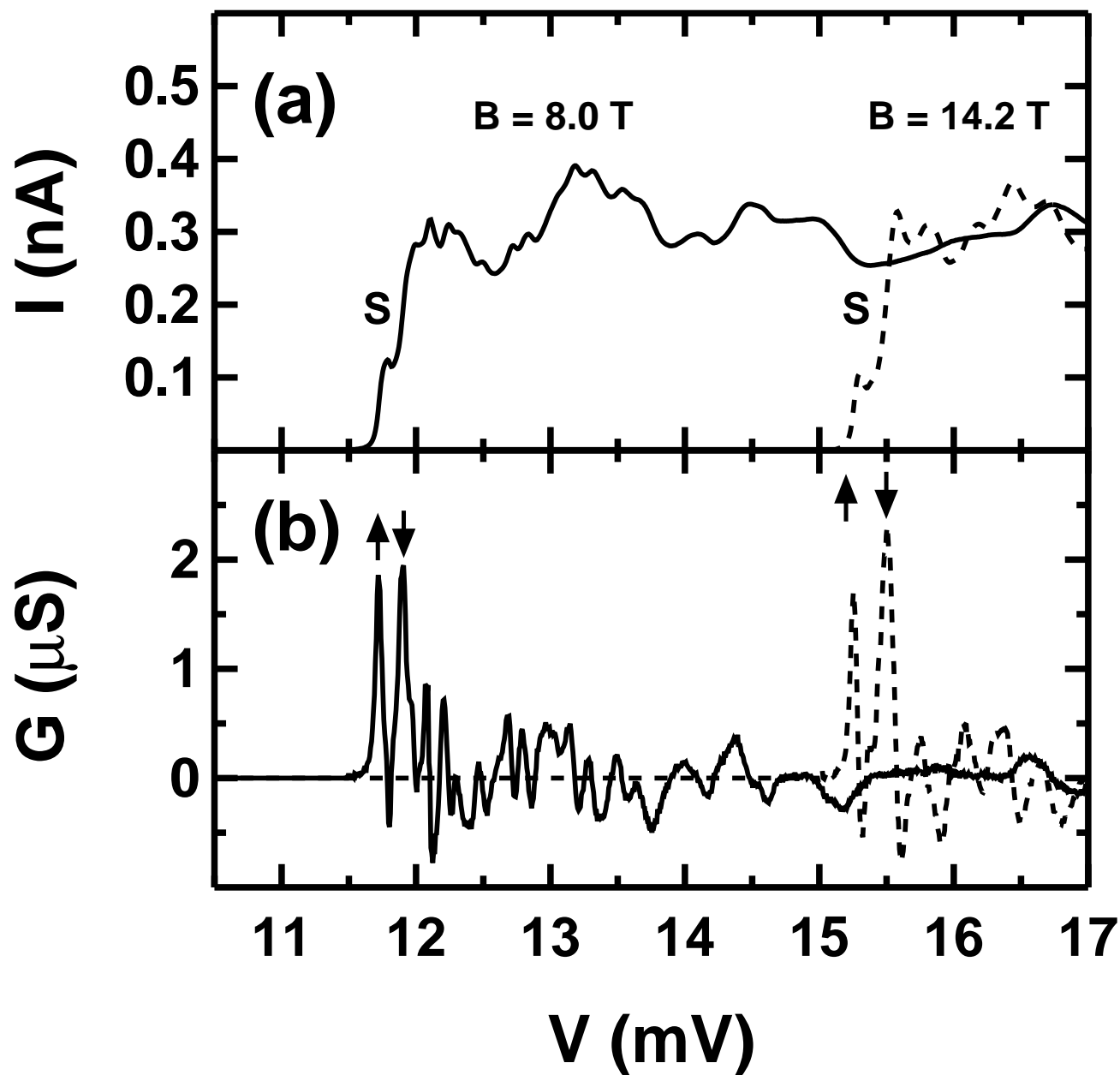
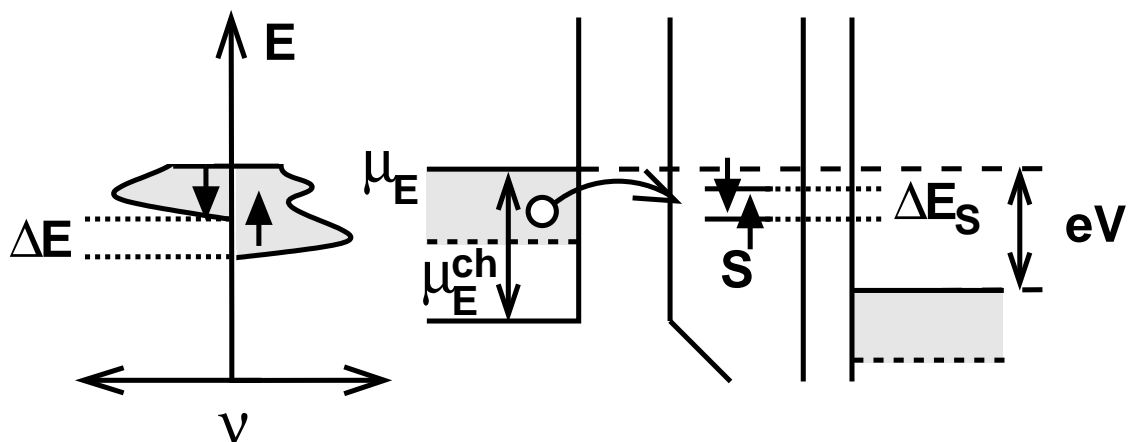


Figure 1, Koenig et al.

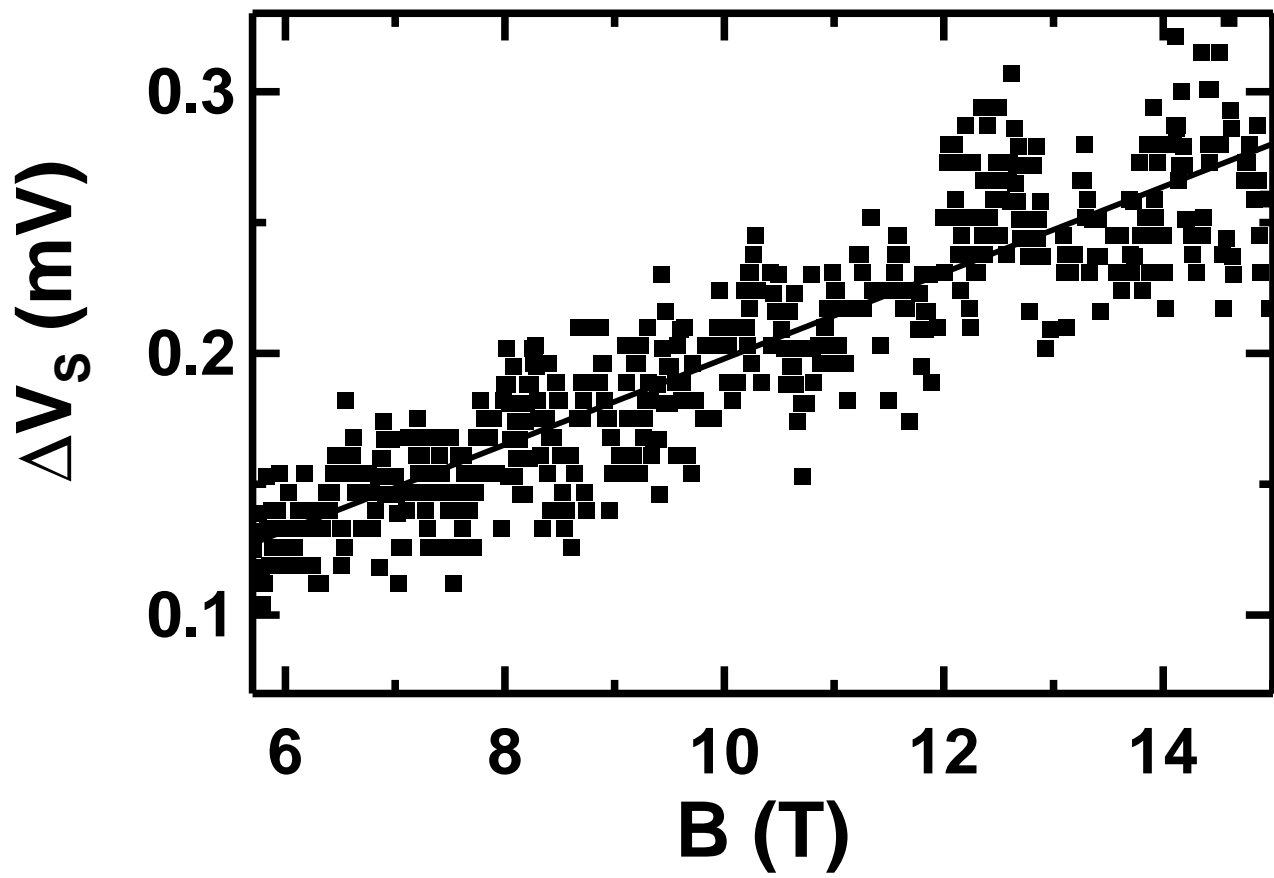


Figure 2, Koenig et al.

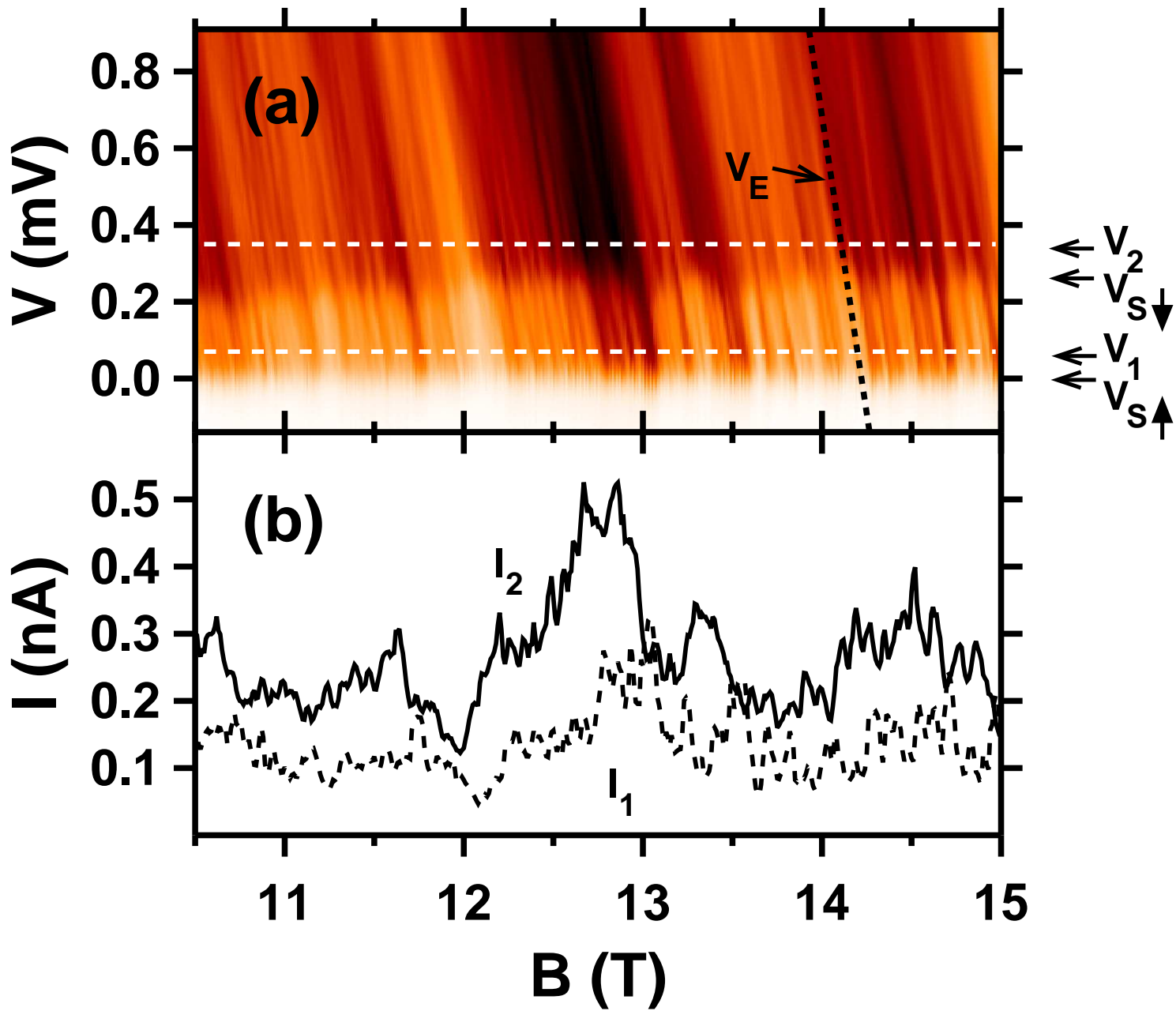


Figure 3, Koenig et al.

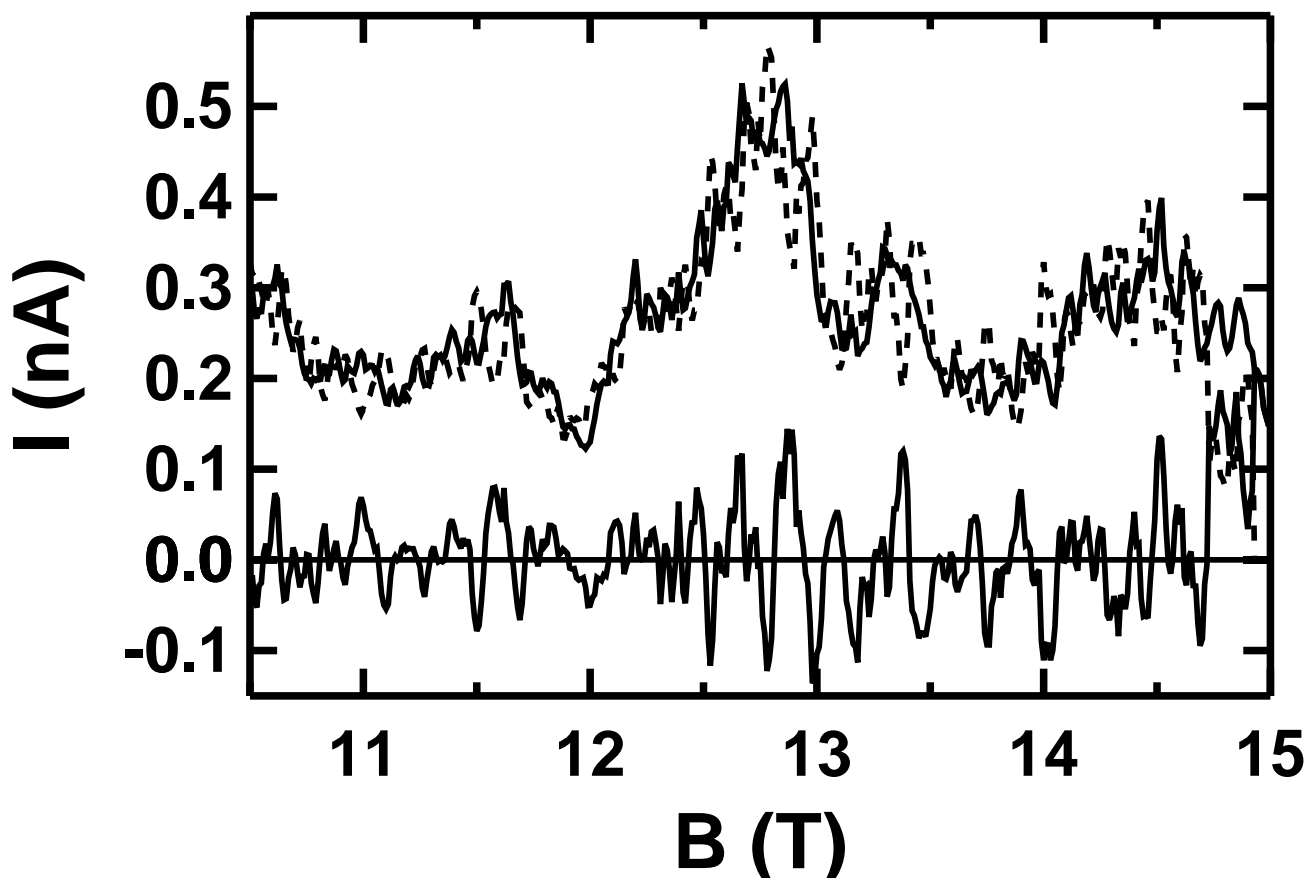
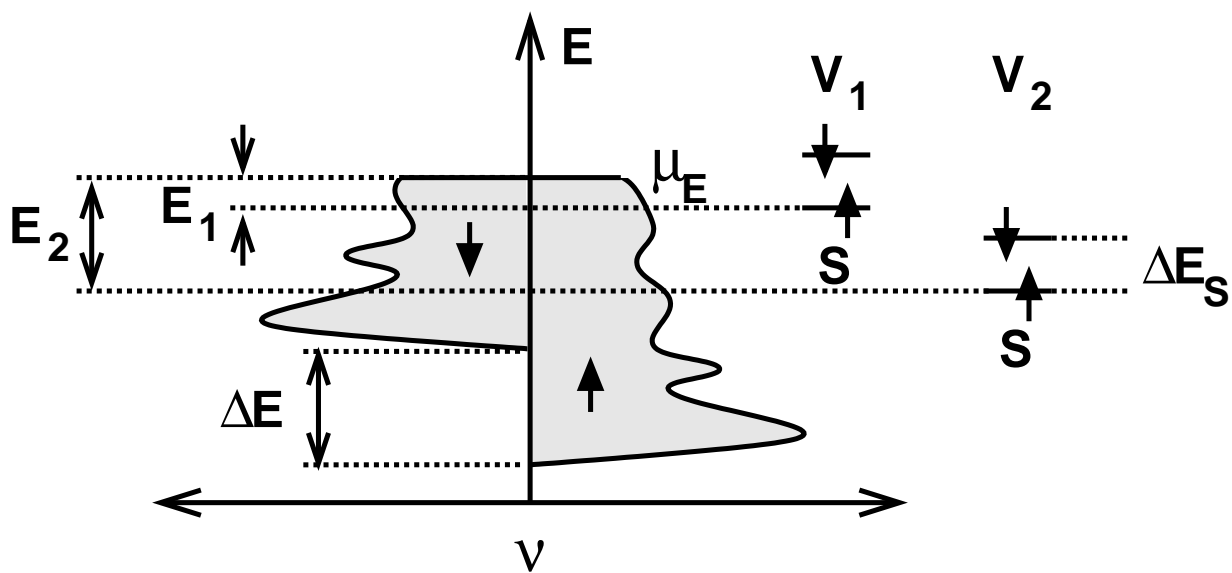


Figure 4, Koenig et al.



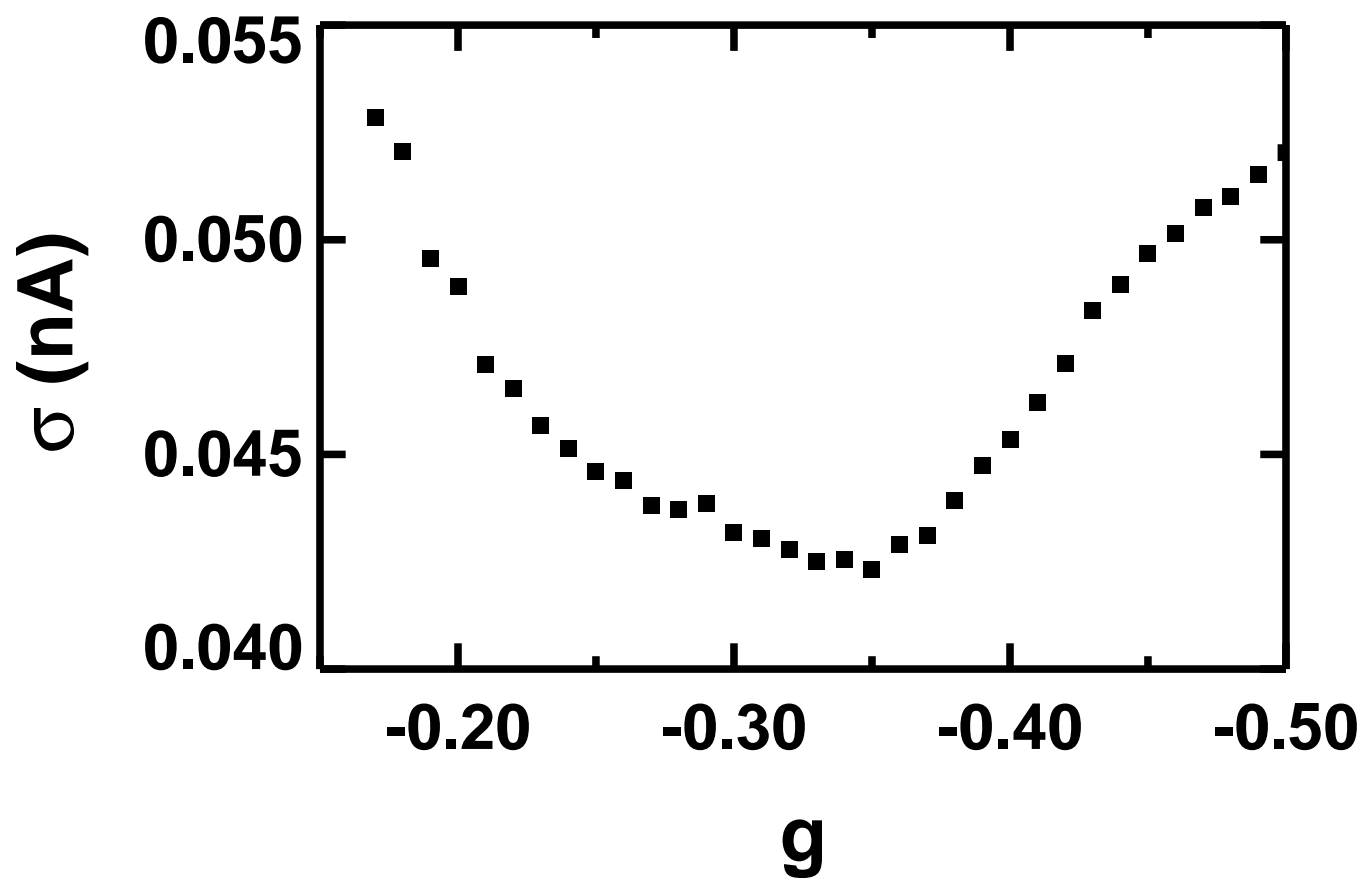


Figure 5, Koenig et al.